A double Gerdien instrument for simultaneous bipolar air conductivity measurements on balloon platforms

K. A. Nicoll, and R. G. Harrison

View Online   Export Citation

ARTICLES YOU MAY BE INTERESTED IN

A computer-controlled Gerdien atmospheric ion counter
Review of Scientific Instruments **71**, 3037 (2000); https://doi.org/10.1063/1.1305511

A lightweight balloon-carried cloud charge sensor
Review of Scientific Instruments **80**, 014501 (2009); https://doi.org/10.1063/1.3065090

Note: A self-calibrating electrometer for atmospheric charge measurements from a balloon platform
Review of Scientific Instruments **84**, 096107 (2013); https://doi.org/10.1063/1.4821500

A double Gerdien instrument for simultaneous bipolar air conductivity measurements on balloon platforms

K. A. Nicoll[a)] and R. G. Harrison
Department of Meteorology, University of Reading, P.O. Box 243, Earley Gate, Reading, Berks RG6 6BB, United Kingdom

A bipolar air conductivity instrument is described for use with a standard disposable meteorological radiosonde package. It is intended to provide electrical measurements at cloud boundaries, where the ratio of the bipolar air conductivities is affected by the presence of charged particles. The sensors are two identical Gerdien-type electrodes, which, through a voltage decay method, measure positive and negative air conductivities simultaneously. Voltage decay provides a thermally stable approach and a novel low current leakage electrometer switch is described which initiates the decay sequence. The radiosonde supplies power and telemetry, as well as measuring simultaneous meteorological data. A test flight using a tethered balloon determined positive (σ_+) and negative (σ_-) conductivities of $\sigma_+ = 2.77 \pm 0.2$ fS m^{-1} and $\sigma_- = 2.82 \pm 0.2$ fS m^{-1}, respectively, at 400 m aloft, with $\sigma_{+}/\sigma_- = 0.98 \pm 0.04$. © *2008 American Institute of Physics.* [DOI: 10.1063/1.2964927]

I. MOTIVATION

The finite conductivity of atmospheric air results from positive and negative cluster ions, created by galactic cosmic rays and Earth's natural radioactivity. The positive (σ_+) and negative (σ_-) air conductivities are both strongly influenced by the presence and charge state of droplets and particles. Measurement of σ_+ and σ_- therefore provides information on electrification, such as at cloud boundaries, where charge-sensitive microphysical processes occur.[1–3] The ratio σ_{+}/σ_- determines the charge distribution on particles.[4] Early aircraft measurements of the conductivity ratio in clear air, between heights of 200 and 5000 m, found an average value of 0.95.[5] However, there are very few conductivity observations in fair weather (nonthunderstorm) cloud regions, and of the measurements existing, almost none measured both polarities simultaneously.

Air conductivity measurements effectively began with Gerdien,[6] who developed a coaxial cylindrical electrode collector, still known as the *Gerdien condenser*. Measurements above the surface used manned balloons,[7,8] followed by development of smaller sensors in the 1950s for use with meteorological radiosondes, which did not have to be recovered after the flight.[9–13] Most of these instruments were flown solely in fair weather conditions in the absence of cloud. The few past conductivity measurements made in cloud have been generally in highly electrified environments during thunderstorms.[14,15]

The fair weather cloud boundary region remains largely unexplored electrically and this paper describes a lightweight balloon based conductivity instrument to measure bipolar air conductivity in fair weather and semifair weather conditions with cloud, but where no strong local charge generation processes are active.

II. DESIGN CONSIDERATIONS

The instrument developed here consists of two symmetrical sampling electrodes based on Gerdien's technique, to measure both polarities of air conductivity simultaneously. It is lightweight ($\sim$150 g) and its low component cost (less than £50 UK), permits it to be used on free balloon flights from which the instruments are not recovered.

A. Dimensions of Gerdien condenser electrodes

In Gerdien's original conductivity instrument,[6] a potential difference was applied between two coaxial cylindrical electrodes, with air drawn between the cylinders. Ions with the same polarity as the outer electrode moved toward the central electrode, and the conductivity inferred from a voltage relaxation measurement. Using two Gerdien condensers, it is possible to measure both positive and negative ions simultaneously. For a compact Gerdien sensor, with geometry largely determined by the radiosonde used, the ion currents are generally small ($\sim$10 fA), requiring an electrometer. To maximize the ion current, the dimensions of the outer and central electrodes and the bias voltage applied between them must be carefully chosen. For an air conductivity σ, the current i to the central electrode due to ions is given by

$$i = \frac{2\pi V L \sigma}{\ln\left(\frac{b}{a}\right)}, \tag{1}$$

where a and b are the radii of the central and outer central cylindrical collecting electrodes, V is the voltage across the electrodes (bias voltage), and L is the length of the tube. The black lines in Fig. 1 show the ion currents calculated from Eq. (1), for unipolar air conductivity values of $\sigma = 1$, 3, and 5 fS m^{-1}, as a function of bias voltage. The electrode dimensions are principally constrained by the size of the radiosonde with which the device is used. For the Vaisala RS80 radiosonde employed, the cuboidal dimensions are
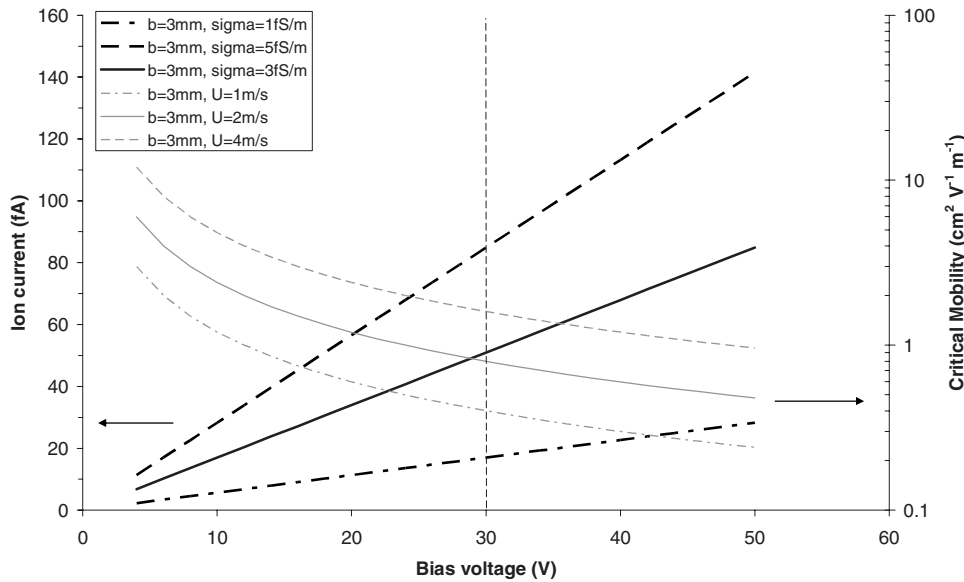
---

a)Electronic mail: k.a.nicoll@reading.ac.uk.

FIG. 1. Calculated ion currents as a function of bias voltage (left-hand axis and black lines) using Eq. (1), assuming air of conductivity $\sigma = 1$, 3, and 5 fS m^{-1}, for a Gerdien instrument having a central electrode radius b =3 mm, outer electrode radius a =15 mm, and length L=145 mm. Calculated critical mobilities (μ_c) as a function of bias voltage (right-hand axis and gray lines) for the same geometry and $\sigma = 5$ fS m^{-1} for ventilation rates, $u = 1$, 2, and 4 m s^{-1} [Eq. (2)]. The vertical dashed line marks the nominal bias voltage (30 V) chosen for the instrument.

$95 \times 145 \times 60$ mm. The maximum electrode length is therefore L=145 mm and the outer and central electrode radii are chosen to be a=15 mm and b=3 mm, respectively. For these dimensions,[3] and a typical surface conductivity of 5 fS m^{-1} (approximately equal to 300 ions cm^{-3}),[16] a bias voltage of 30 V produces an ion current of ~80 fA, which does not overly constrain the electrometer leakage required.

The ventilation rate determines the mobility of ions detected. Only the smallest, fastest ions (which in the lower atmosphere have mobilities spanning 0.5–3 cm^2 V^{-1} m^{-1}) (Ref. 17) contribute to the majority of the air's conductivity. For a Gerdien condenser, the most important ion parameter is the critical mobility μ_c, which determines the smallest mobility ion measured. It is defined as

$$\mu_c = \frac{(b^2 - a^2)\ln\left(\frac{b}{a}\right)u}{2VL}, \qquad (2)$$

where u is the ventilation rate inside the tube. The gray lines in Fig. 1 show μ_c as a function of bias voltage. For a bias voltage of 30 V and a ventilation rate of 2 m s^{-1}, μ_c =0.8 cm^2 V^{-1} m^{-1}.

B. Selection of relaxation technique

Gerdien condensers have been previously used to find σ either directly by current measurement, or as with the original Gerdien method, through using the rate of change in electrode voltage to infer the ion current flowing. A disadvantage of the current measurement mode for a disposable atmospheric instrument is that it requires expensive high value (~10^{12} Ω) resistors, which may have appreciable temperature coefficients. The instrument described therefore uses the voltage relaxation method to avoid the need for a high value resistor. The approach used is to reset the central electrode voltage to a known value and determine the rate of change in voltage. After a set number of measurements, the central electrode voltage is reset and the cycle repeated. Previous implementations of voltage decay measurements have used mechanical switches to reset the electrode voltage,[11] but

a compact solid-state electrometer switch system is implemented here for reliability at low temperatures.

C. Electrometer switch considerations

The voltage measurement is made with a simple electrometer operational amplifier follower circuit, with a junction field effect transistor (j-FET) diode acting as a switch to reset the electrode voltage. In fact, two j-FETs are wired in inverse parallel—hereafter referred to as a bi-directional j-FET electrometer diode (BjED)—to enable bipolar current flow, which was found in practice to readily facilitate recovery from fault conditions. The essential requirements of the j-FETs chosen are that for a small gate-source voltage (V_{gs}), the gate-source current (i_{gs}) must be appreciably less than the ion current.

Figure 2 shows the basic implementation. During the voltage decay measurements the changeover switch is in the "measure" position and the BjED acts as a blocking element. In the "reset" position, the BjED conducts and the central
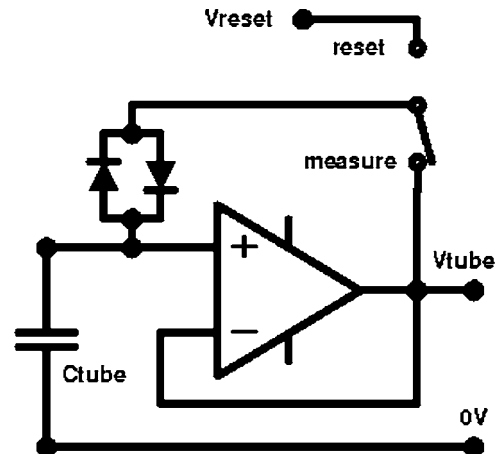

FIG. 2. Basic implementation of the electrometer and reset switch used for positive and negative electrodes. The inverse parallel diodes are implemented using j-FET transistors, which act as a low leakage switch to charge C_{tube} to V_{reset}.
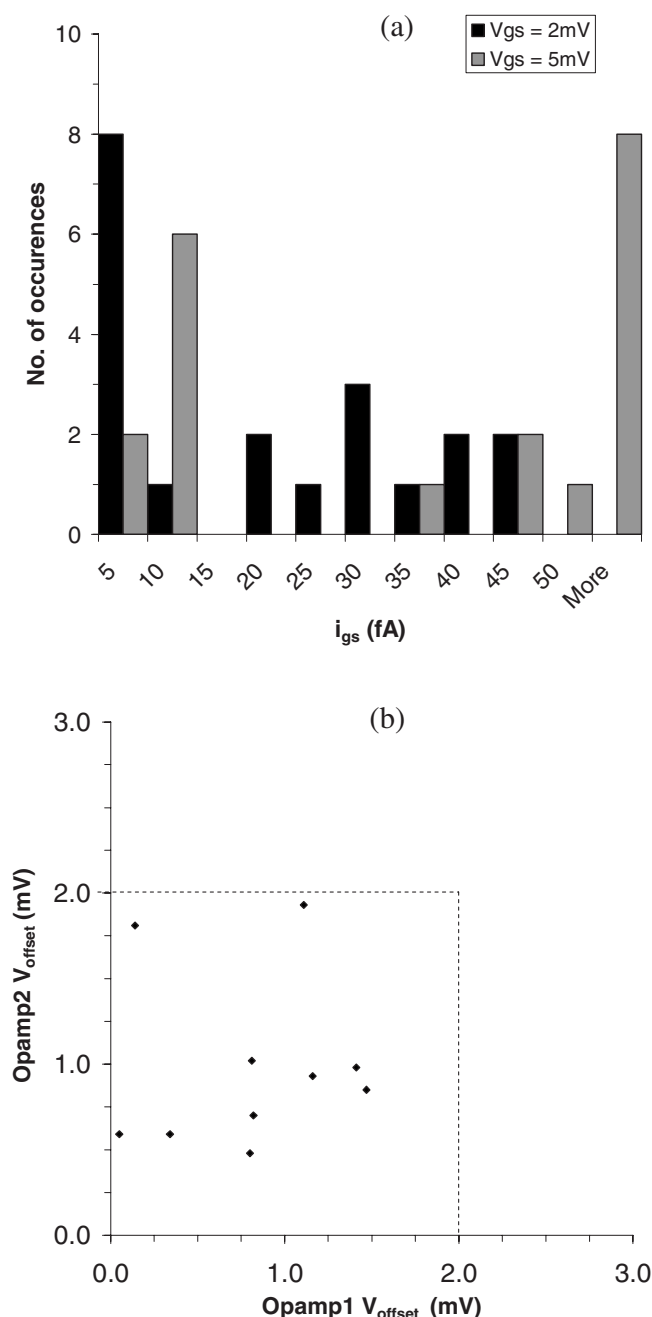
FIG. 3. (a). Histogram of the gate-source current, i_{gs} measured for 20 J113 j-FETs at $V_{gs}=2$ mV (black bars) and $V_{gs}=5$ mV (gray bars). (b) Offset voltages for each of the paired opamps in a sample of ten LMC6042 dual opamps. The dotted line represents $V_{offset}=2$ mV.

electrode voltage becomes V_{reset}. The reset voltage is normally set to 2 V for the positive Gerdien condenser and 5 V for the negative one.

To minimize leakage currents during voltage measurements it is essential that the offset voltage, V_{offset}, of the operational amplifier (opamp), which determines the j-FET gate-source voltage, V_{gs}, is minimized. The opamp selected, a National semiconductor LMC6042, has a typical offset voltage of ~ 2 mV. The V_{gs}-i_{gs} response characteristic was measured for a sample of type J113 j-FETS, using a Keithley 6512 electrometer. Histograms of i_{gs} for $V_{gs}=2$ mV and $V_{gs}=5$ mV are displayed in Fig. 3(a). For $V_{gs}=2$ mV, 40% of

the i_{gs} are less than 5 fA, however 50% cause $i_{gs} > 20$ fA. For $V_{gs}=5$ mV, 40% have $i_{gs} < 10$ fA but the majority permits current flow of >50 fA. From Fig. 1, $i_{gs} < 8$ fA is required to contribute less than 10% error to the current measurements. This can be achieved for the large majority of j-FETs sampled when $V_{gs}=2$ mV but not when $V_{gs}=5$ mV.

The requirement for $V_{gs} \leqslant 2$ mV necessitates further investigation of the opamp used. The LMC6042 opamp is primarily selected for its low leakage current ($i_b \sim 2$ fA) and because it is a dual device, it enables two channels to be measured simultaneously with one device package. To investigate the offset voltage characteristics of two opamps within the same package, the offset voltages were measured for a sample of ten LMC6042s and are plotted against each other in Fig. 3(b). The lack of linearity shows variation in the V_{offset} between the two channels of the dual opamp, although neither opamp in the package performs consistently better than the other. All measured offset voltages were less than 2 mV, implying that for any LMC6042 chosen at random, both opamp channels will have sufficiently small V_{offset} for the j-FET i_{gs} to permit the instrument to operate. It is clear that the component to component variation in V_{offset} can be neglected.

III. FLIGHT PACKAGE

A. Circuitry

Figure 4 shows the circuit diagram of the electronic system utilized for measuring the Gerdien condenser ion currents. The circuitry immediately around the opamp stages implements the principles explained in Fig. 2 through using the double j-FET configuration of electrometer diodes, a dual opamp, and metal oxide semiconductor FET (MOSFET) changeover switches. It is used with the four channel radiosonde data acquisition system previously described,[18] which provides an 18 V supply, timed reset pulses, and 12 bits analog to digital voltage conversion. The circuit provides a bias voltage to the outer electrode of each Gerdien condenser, of $\sim +30$ V (positive conductivity Gerdien condenser) and ~ -30 V (negative conductivity Gerdien condenser). This is produced by the power supply modules PSU1 and PSU2, from the 12 V regulated supply from IC4. R9 and R10 provide short circuit protection for the bias generators.

The rate of voltage change on the well-insulated central electrode is used to determine the ion current, employing similar circuitry for both Gerdien condensers. For the positive conductivity tube, an $\sim +30$ V bias is applied to the outer electrode. The voltage on the tube's central electrode is measured using the electrometer voltage follower formed by IC2a, via R5, air wired to the input pin on IC2a to maintain high insulation resistance. R5 provides basic overvoltage protection to IC2a. IC2 is powered from a +12 V supply, hence its output range can span up to 12 V. A potential divider (R6 and R7) is used to reduce its output to the 0–5 V range required by the analog to digital converter of the radiosonde data acquisition system, and in addition, C3 and R7 form a low-pass filter.

Before the rate of voltage change is measured, the central electrode potential is reset to a fixed initial voltage, de-
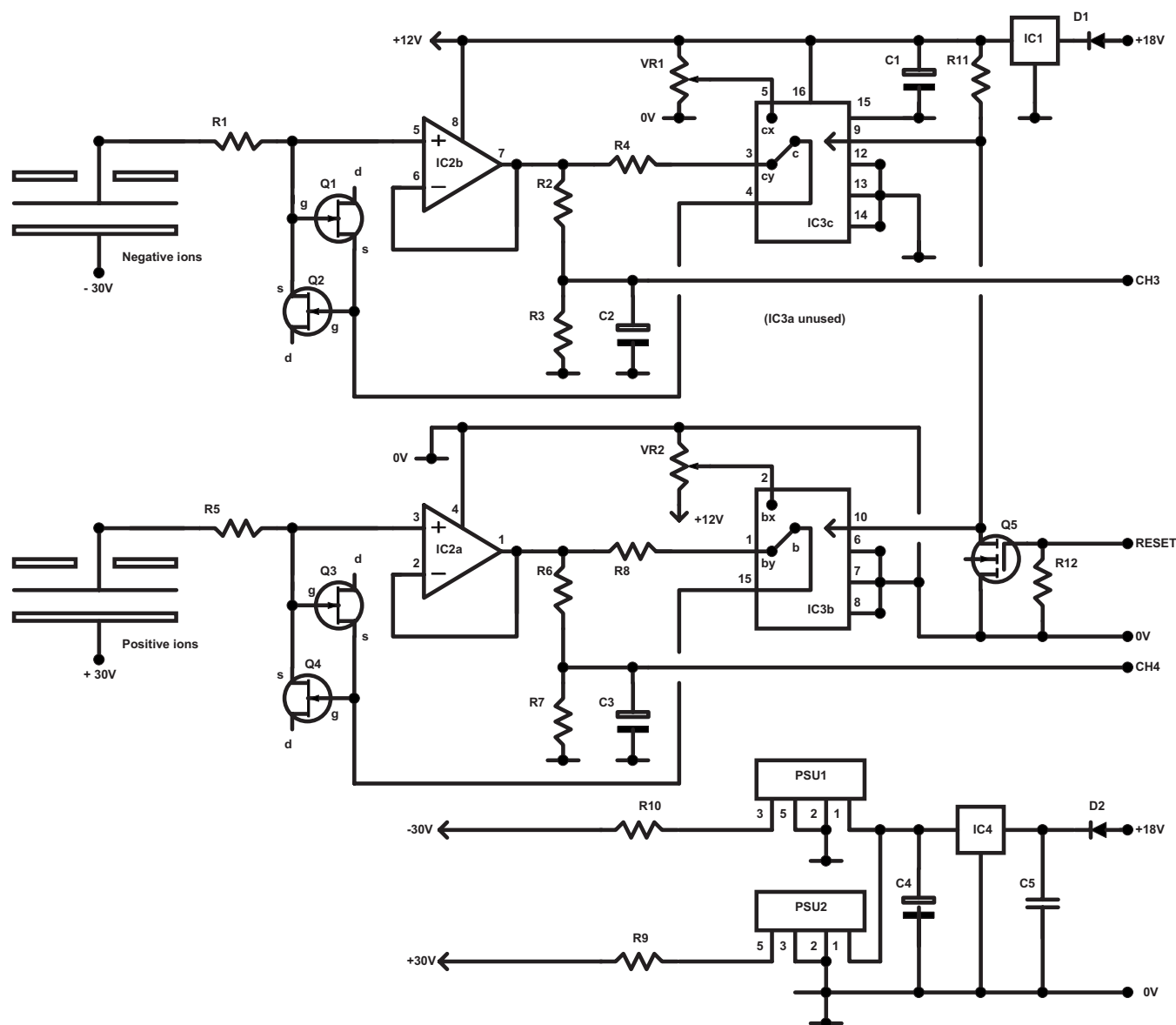
FIG. 4. Circuit diagram for the double voltmeter electrometer, reset switches and bias voltage generators used with the double Gerdien conductivity sensor. A +18 V supply is provided by the radiosonde battery and the electrometer output voltage is connected to channels 3 and 4 (CH3 and CH4) of the radiosonde data acquisition system, programed to provide a reset signal every 100 s. (Components: Q1, 2, 3, 4 J113 j-FET transistors; Q5 VN10LP n-channel MOSFET, IC1 78L12 12 V regulator; IC2 LMC6042 dual electrometer opamp; IC3 4053BE triple changeover MOSFET switch; PSU1, 2 30 V power supply modules type 1A1215S, D1, 2 BAT85 diodes, R1,5 1 MΩ resistors, R2, 6, 9, 10 10 kΩ resistors, R3, 7 6.8 kΩ resistors, R4,8 1 kΩ resistors, R11,12 100 kΩ resistors, C1,4 1 μF capacitors, C2,3 10 μF capacitors, C5 100 nF capacitor).

rived from potentiometer VR2. This initial potential is applied to the central electrode when the reset line is taken high by the data acquisition system. This reset signal causes the MOSFET changeover switch (IC3b) to connect the central electrode to VR2 via the BjED Q3–Q4; as a result of which the central electrode charges to a potential close to the potentiometer voltage. When the reset signal is removed, the changeover switch (IC3b) operates and connects Q3–Q4 to the output of IC2a, via R8. As there is negligible voltage drop across R8, the potential on the IC3b side of Q3–Q4 is, to within the offset voltage of IC2a, equal to the potential at IC2a. As only a small potential difference equal to IC2's offset voltage exists across Q3–Q4, only an ultrasmall leakage current flows and the current flowing is dominated by the ion current within the Gerdien condenser. An identical approach is implemented with the negative conductivity tube, using voltage follower IC2b, changeover switch IC3c, and BjED Q1–Q2. The two changeover switches IC3b and IC3c are driven together via Q5, to provide level shifting from the data acquisition system.

For the apparatus to work, the essential requirements, as mentioned, are that IC2 has ultralow bias current and low offset voltage. However, the data sheet for the chosen opamp (type LMC6042) shows that it is stable into capacitive loads of less than 100 pF. R4 and R8 act to isolate the capacitance presented by the Gerdien condensers and BjED devices, with no instability apparent. The total current consumption of the circuit is ~22 mA, the majority due to the bias voltage generators PSU1 and PSU2.
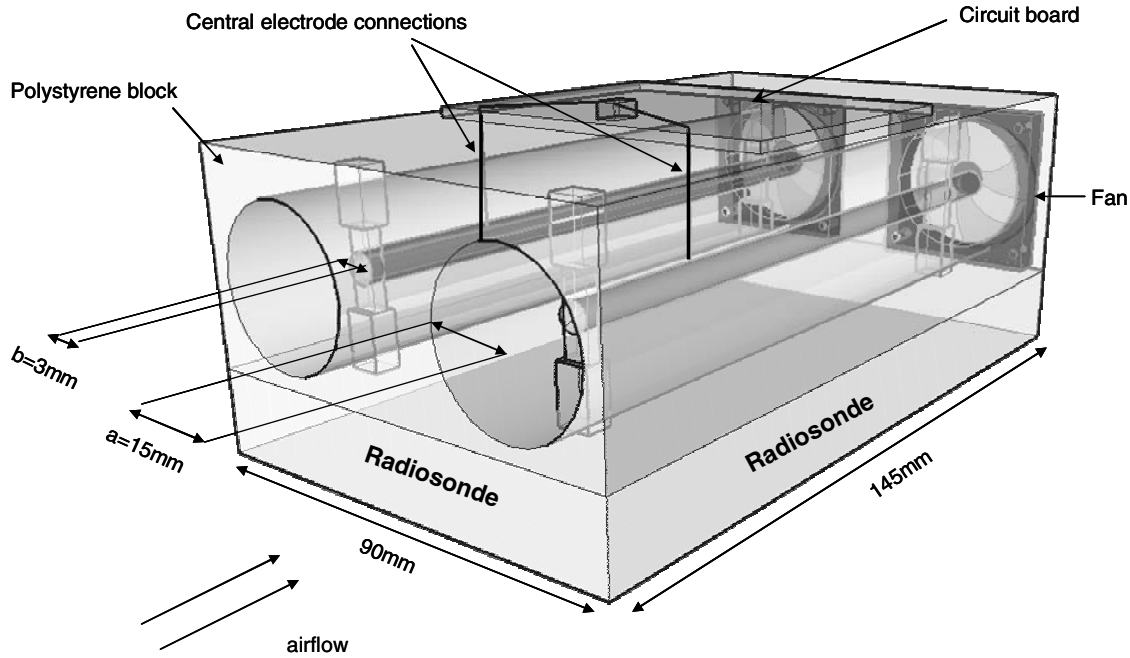
FIG. 5. Cutaway diagram of double Gerdien conductivity apparatus attached to a standard meteorological radiosonde (Vaisala type RS80). Both Gerdien condensers are mounted inside a single polystyrene block, with a fan (RS type: Maglev $30 \times 30 \times 6$ mm^3) attached to the exit port of each tube. Each tube's central electrode is secured by two vertical PTFE struts and the connection from the central electrode to the circuit board is air wired via a PTFE insulated hole in the polystyrene.

B. Deployment

Each outer electrode consists of a cylinder wound from 0.25 mm thick copper foil, length of 145 mm, and radius of 15 mm. The central electrode is made from 3 mm radius hollow copper tubing and length of 125 mm. Both Gerdien condensers are secured inside a 90×145 mm^2 block of polystyrene, with the circuit board mounted on top, inside a screening metal box. The connection from the central electrode to the electrometer is made through a polytetrafluoroethylene (PTFE) lined hole in the polystyrene, directly air wired to the circuit board. The connecting wire is kept short to minimize stray capacitances.

Each Gerdien condenser is force ventilated by a 5 V dc fan, secured at the exit end of the tube, and powered by 2 $\times$ AAA batteries. These provide a ventilation rate of $\sim$2 m s^{-1} inside each tube. Figure 5 shows a diagram of the conductivity instrument.

During flights, the conductivity apparatus is mounted on the side of a Vaisala RS80 radiosonde, to enable pressure, temperature, humidity, and geographical position to be recorded synchronously with the conductivity measurements. The voltage on each central electrode is sampled at 1.3 Hz and central electrode voltage resets are programed via the digital acquisition system, to occur every 100 s, of 5 s duration. The central electrode voltages are also measured throughout the reset period. The meteorological data are logged in the standard way using a Vaisala PP11 decoder and laptop. The two channels of conductivity data are logged using a separate laptop and the data files are merged through prior synchronization of the laptop real time clocks. Further data processing separates the merged data file into a set of individual cycle files, one for each measurement cycle con-

taining time stamp, measurement number, and the two central electrode voltage measurements.

IV. DATA ANALYSIS

To calculate air conductivity from a Gerdien condenser in voltage measurement mode, an exponential fit to the voltage decay/increase on the central electrode is normally applied[16] and the conductivity calculated from the exponential time constant. For short portions of exponential change, a linear change can be assumed. For each Gerdien condenser, the ion current, i, is calculated from the rate of change in central electrode voltage with time, dV_c/dt, using the following formula:

$$i = (C_g + C_m)\frac{dV_c}{dt}, \qquad (3)$$

where C_g is the capacitance of the Gerdien condenser and C_m is the capacitance of the measuring system. dV_c/dt is obtained by applying a linear least squares fit to the time series of voltage measurements. The polar air conductivity, σ_+ or σ_-, is calculated from

$$\sigma_\pm = \frac{i\varepsilon_0}{C_g(V_{b\pm} - V_{c\pm})}, \qquad (4)$$

where $\varepsilon_0 = 8.85 \times 10^{-12}$ F m^{-1} and $V_{b\pm} - V_{c\pm}$ is the difference between the outer, V_b, and central electrode voltage V_c (i.e., the effective bias voltage between the two electrodes). The slight difference in effective bias voltages leads to a difference in μ_c between the two Gerdien condensers, but as Fig. 1 shows, this effect is small. Equation (4) requires the Gerdien capacitance C_g and Eq. (3) requires C_m. By experiments without the condenser present, C_m was found to be $<5\% C_g$,
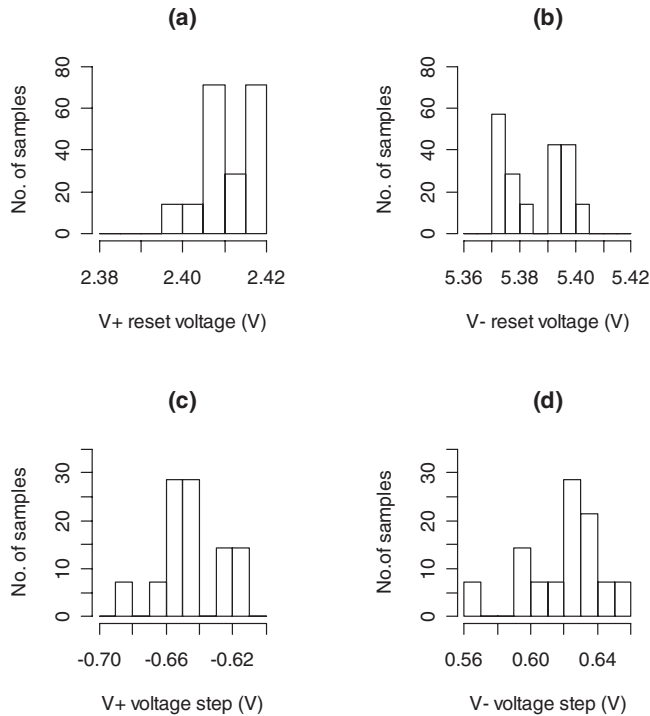
(a)

(b)

(c)

(d)

FIG. 6. Results obtained during a test flight made from a tethered balloon. (a) and (b) show histograms of the central electrode reset voltages for (a) the positive (V_+) and (b) negative (V_-) conductivity Gerdien tubes. (c) and (d) show the voltage step between the reset voltage and the first measurement in a cycle, for (c) the positive and (d) negative Gerdien tubes, indicating that charge injection takes place after each reset event.

hence, combining Eq. (3) and (4), and assuming that $C_m \ll C_g$, $\sigma_\pm$ can be calculated independently of C_g, from

$$\sigma_\pm = \frac{\varepsilon_0}{(V_{b\pm} - V_{c\pm})}\left[\frac{dV_{c\pm}}{dt}\right]. \tag{5}$$

V. RESULTS AND DISCUSSION

The instrument and receiving equipment were tested using a 20 m^3 helium filled tethered surveillance balloon flown at Chilbolton Observatory, Hampshire, UK, in April 2008. The conductivity apparatus was hung approximately 20 m beneath the balloon using a nylon rope. During the flight, the weather conditions were dry, with full cloud cover, but the balloon remained below cloud base throughout. Before the launch, the balloon was maintained at a constant height of 20 m for 90 min, to allow any excess charge on its surface to come into equilibrium with its surroundings. (The relaxation time constant for the balloon is determined by σ/ε_0, $\sim$1500 s). This procedure also enabled dissipation of any electrostatic charge present on the insulators. A further precaution to prevent effects of balloon charge was to orient the Gerdien condensers horizontally which shielded the central electrodes from any remaining charge on the balloon vertically above.

During the measurements which follow, the balloon was rising at about 0.1 ms^{-1}, between 300 and 520 m above the surface. Figures 6(a) and 6(b) show histograms of the reset voltages on the positive (V_+) and negative (V_-) central electrodes, respectively. On average the positive channel was re-

set to 2.41 V and the negative channel was reset to 5.39 V. The small spread in the reset voltages on both channels shows consistent reset switch operation throughout the flight.

To investigate charge injection at the end of the reset switching, the voltage step between the last reset period measurement and the first nonreset measurement was extracted. Histograms are shown in Figs 6(c) and 6(d), for the positive (V_+) and negative central electrodes (V_-), respectively. After each reset, the positive electrode voltage drops by an average of 0.64 V. Calculating a Gerdien capacitance of 5.2 pF from geometry considerations, this voltage step corresponds to charge injection of −3.3 pC. The voltage on the negative electrode increases by 0.62 V after reset, equivalent to charge injection of +3.3 pC. Ultimately, this charge injection does not affect the measurement of conductivity as long as the voltage decay is measured after the charge injection is completed, as a substantial initial voltage is still established on the central electrode.

The raw voltage measurements and derived ion currents, using Eq. (3), are shown in Fig. 7. The solid squares near the top of the plot denote central electrode voltage measurements. Each cycle of electrode voltage measurements is separated by a series of reset voltage measurements, represented by hollow squares. It is clear that the reset voltages on each central electrode are approximately constant throughout the duration of the flight. The rate of change in voltage is similar in most cycles, indicating that there is very little leakage through the PTFE insulators; the presence of water films on the insulators has been observed to cause catastrophic failure, therefore the consistent behavior from one cycle to another indicates negligible moisture effects. The two lower traces show the magnitude of positive (solid gray circles), and negative ion currents (solid black circles), i_+ and i_-, calculated from Eq. (3), using a Gerdien condenser capacitance of 5.2 pF. The traces track each other fairly closely, and the median values of i_+ and i_- are 55.5 ± 3.1 and 70.6 ± 4.6 fA, respectively.

Figure 7(b) shows the experimentally determined ion current magnitude from Fig. 7(a), plotted against the effective bias voltage, with part of the theoretical calculations of Fig. 1 included. The measured ion currents were calculated from the voltage measurements in Fig. 7(a), using Eq. (3), binned into 0.5 V intervals and averaged. The effective bias voltages are given by $V_{b\pm} - V_{c\pm}$, where V_b is the outer electrode voltage ($\pm$32 V) and V_c is the central electrode voltage. Thus, the magnitudes of the effective bias voltages on the positive and negative condensers are $\sim$28 and 36 V, respectively. It is clear that the points cluster between the $\sigma = 3$ fS m^{-1} and $\sigma = 5$ fS m^{-1} lines, which are within the range of conductivities typically measured.[16] From Eq. (1), the gradient of ion current plotted against bias voltage is related to the mean conductivity. The gradient of a fitted line to the measured ion current values is 1.7 ± 0.7 fA V^{-1}, giving a mean conductivity of 2.9 ± 1.3 fS m^{-1}

Figure 7(c) shows a histogram of derived positive and negative conductivites from Eq. (5), using the data from Fig. 7(a). The mean ratio of σ_+/σ_- is 0.98 ± 0.04. The median values of σ_+ and σ_- are 2.77 ± 0.16 and 2.82 ± 0.18 fS m^{-1}, respectively, with two standard errors quoted.

(a)

(b)   **(c)**
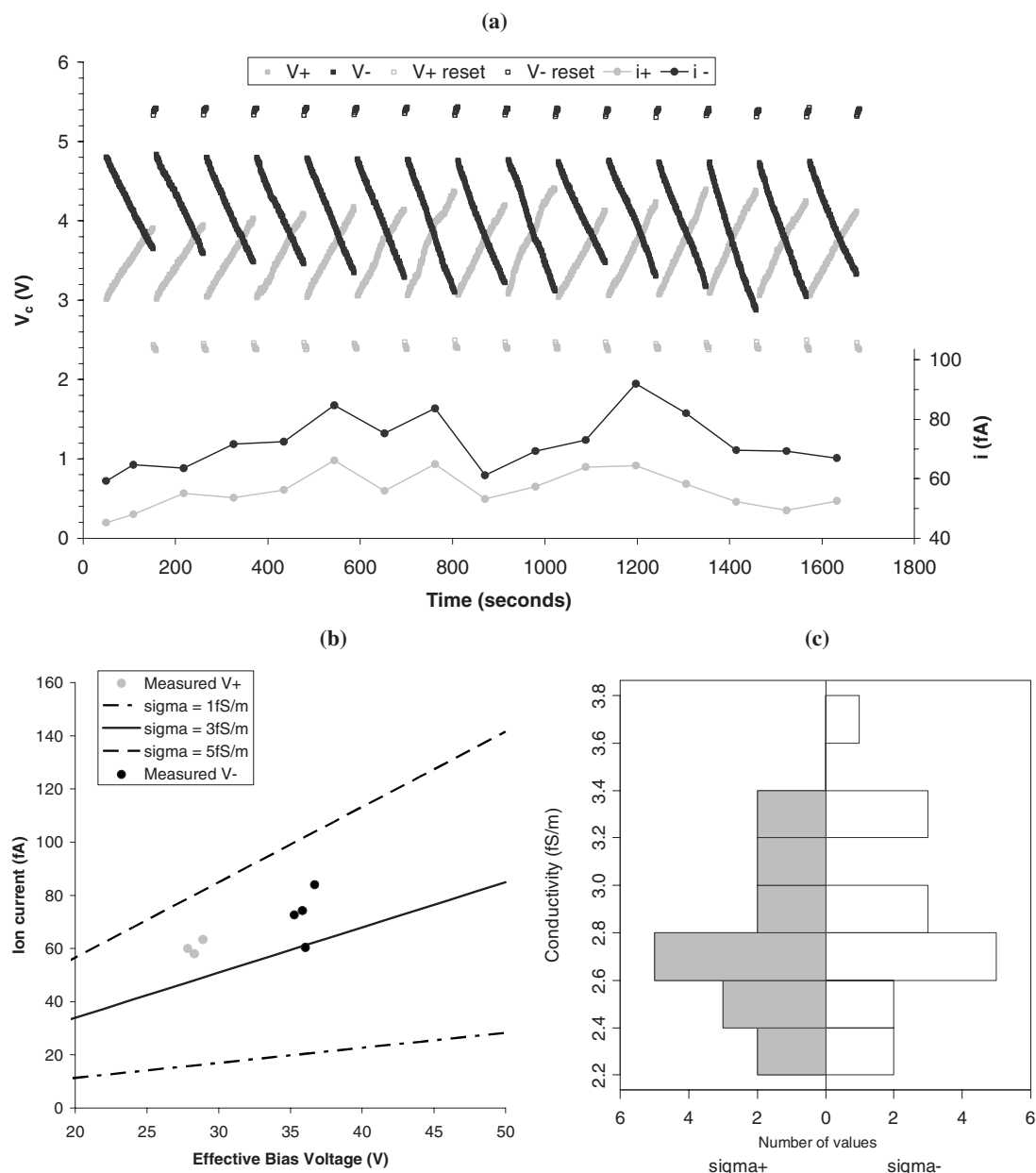

FIG. 7. (a) Time series of central electrode voltage measurements V_c from a series of operating cycles (left-hand axis). Solid squares denote samples during the measurement part of the cycle from the positive (gray points) and negative (black points) Gerdien condenser; hollow squares denote samples during the reset part of the cycle. The right-hand axis and solid circles show the magnitude of the ion currents derived from the voltages using Eq. (3), assuming a Gerdien capacitance of 5.2 pF. (b) Magnitudes of the ion currents from (a) plotted against the effective bias voltage (positive condenser grey points, negative condenser black points), overplotted on a portion of the calculated ion currents from Fig. 1 (black lines). [Ion currents were calculated from the voltage measurements in (a), using Eq. (3), binned into 0.5 V intervals and averaged.] (c) Histogram of positive (left side, gray bars) and negative (right side, white bars) air conductivities, derived from the data in (a) using Eq. (5).

Measurements made with the instrument immediately above the surface, where electrode effects enhance positive ion concentrations,[19] gave a ratio of $\sigma_+/\sigma_- = 1.47 \pm 0.26$, larger than that observed aloft at ~ 400 m. This demonstrates that the instrument is capable of measuring a range of conductivity ratios.

[1] K. S. Carslaw, R. G. Harrison, and J. Kirkby, Science **298**, 1732 (2002).
[2] L. Zhou and B. A. Tinsley, J. Geophys. Res. **112**, 11203 (2007).
[3] R. G. Harrison and M. H. P. Ambaum, Proc. R. Soc. London, Ser. A (unpublished).
[4] R. Gunn, J. Meteorol. **11**, 339 (1954).
[5] R. C. Sagalyn, *Recent Advances in Atmospheric Electricity*, edited by, L. G. Smith (Pergamon Press, Portsmouth, New Hampshire, 1958), p. 235.
[6] H. Gerdien, Nachr. Ges. Wiss. Goettingen, Math.-Phys. Kl., 240 (1905).
[7] A. Wigand, J. Terr. Magn. Atmos. Elect. **19**, 93 (1914).
[8] O. H. Gish and K. L. Sherman, Nat. Geog. Soc. Tech. Papers **2**, 94 (1936).
[9] R. H. Woessner, W. E. Cobb, and R. Gunn, J. Geophys. Res. **63**, 171 (1957).
[10] H. Hatakeyama, J. Kobayashi, T. Kitaoka, and K. Uchikawa, *Recent Advances in Atmospheric Electricity*, edited by L. G. Smith (Pergamon, Portsmouth, New Hampshire, 1958), p. 119.
[11] S. Venkiteshwaran, *Recent Advances in Atmospheric Electricity*, edited by

L. G. Smith (Pergamon, Portsmouth, New Hampshire, 1958), p. 89.

[12] G. W. Paltridge, J. Geophys. Res. **70**, 2751 (1965).

[13] Y. Morita, H. Ishikawa, and M. Kanada, J. Geophys. Res. **76**, 3431 (1971).

[14] J. P. Scott and W. H. Evans, Pure Appl. Geophys. **75**, 219 (1969).

[15] W. D. Rust and C. B. Moore, Q. J. R. Meteorol. Soc. **100**, 450 (1974).

[16] K. L. Aplin and R. G. Harrison, Rev. Sci. Instrum. **71**, 3037 (2000).

[17] U. Hõrrak, J. Salm, and H. Tammet, J. Geophys. Res. **105**, 9291 (2000).

[18] R. G. Harrison, Rev. Sci. Instrum. **76**, 12611 (2005).

[19] J. A. Chalmers, *Atmospheric Electricity*, 2nd ed. (Pergamon, Oxford, 1967).